NONLINEAR-FEEDBACK VEHICLE TRACTION FORCE CONTROL WITH LOAD TRANSFER

Annalisa Scacchioli[*]
Department of Aerospace Engineering
Georgia Institute of Technology
Atlanta, Georgia,30309

Panagiotis Tsiotras[†]
Department of Aerospace Engineering
Georgia Institute of Technology
Atlanta, Georgia, 30309

Jianbo Lu[‡]
Research and Advanced Engineering
Ford Motor Company
Dearborn, Michigan, 48124

ABSTRACT

This article deals with the nonlinear feedback regulation of the longitudinal traction forces for high-speed vehicles, possibly over a low friction surface. Hybrid models of the longitudinal vehicle dynamics incorporating load transfer effects, a crucial element in advanced driving techniques, are derived. The designed hybrid regulator allows the tracking of a given friction force profile in the presence of known disturbances and unknown model uncertainties. Simulations show good performance of the proposed hybrid regulator under all operating conditions.

INTRODUCTION

Accident avoidance is the primary task of automotive active safety systems. During an imminent collision, when the driver's reaction time is rather limited, the full utilization of the vehicle's handling capability becomes critical. Only expert drivers are masters of controlling the vehicle at these extreme regimes. Incorporating expert driving skills in an active safety system is an important step forward in the technology of future accident avoidance systems. By fully utilizing the vehicle's handling capability one should be able to stop the vehicle faster or to move the vehicle away from a hazard, thus improving vehicle response to levels that are not possible by novice drivers.

Several contributions have been developed in the last years to improve vehicle control stability. Anti-lock braking systems (ABS) and traction control or acceleration slip regulation (ASR), are examples of the current state of technology. However, to the best of our knowledge, none of these works deals with expert driver-inspired vehicle active safety systems for vehicles in the limit of their handling conditions.

In this article, following our previous works [7, 9, 10], we develop a hybrid model of a vehicle during "left foot braking" a specific driving technique used by rally drivers, which takes advantage of the load transfer effect from front to rear axles and vice versa, to control the friction forces at the front and rear wheels. Specifically, in this technique the driver applies braking and acceleration commands simultaneously in order to fine tune the total torque applied to the wheels.

We describe the system's behavior at two levels of abstraction (the wheels and the vehicle) through a finite number of discrete states and state transitions. We use a family of continuous models incorporating the load transfer effect, within the individual discrete states. Continuous control laws, based on the nonlinear output regulation theory and tracking a given friction force profile, are designed at the highest abstraction level, but implemented at the more accurate, lower wheel abstraction level.

PROBLEM FORMULATION

Vehicle Model

We consider a vehicle in a straight driving condition as shown in Figure 1. We assume that the vehicle lateral load transfer is zero and the road surface friction is evenly distributed on the right and left wheels. The four wheel vehicle can, then, be modeled through a two-wheel bicycle model as shown in Figure 1. Let $\xi = (v, \omega_F, \omega_R)^T$ be the state of the vehicle, where v is the translational velocity (measured along the longitudinal direction of the vehicle) of the center of mass, with ω_F and ω_R the

[*]Email address: annalisa@gatech.edu.
[†]Email address: tsiotras@gatech.edu.
[‡]Email address: jlu10@ford.com.

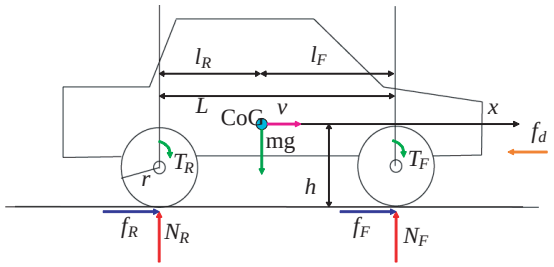

Figure 1. LONGITUDINAL FORCE DISTRIBUTION ON A TWO-AXLE VEHICLE ON A LEVEL ROAD.

angular velocities of the front and rear wheels, respectively. The equations of motion of the vehicle are

$$m\dot{v} = f_F + f_R - f_d, \tag{1a}$$
$$I_F\dot{\omega}_F = T_F - r f_F, \tag{1b}$$
$$I_R\dot{\omega}_R = T_R - r f_R, \tag{1c}$$

where f_F [N] and f_R [N] are the tractive friction forces acting on the front and rear wheels, respectively, f_d [N] is the external disturbance, m [kg] is the mass of the vehicle body, I_F [kgm^2] and I_R [kgm^2] denote the rotational moments of inertia of the front and rear wheels, respectively, and r [m] is the rolling radius of the wheels. Furthermore, T_F [Nm] is the total torque (engine drive torque and brake torque) acting on each of the front wheels, while T_R [Nm] is the total torque acting on each of the rear wheels. Without loss of generality, we assume a FWD (Front Wheel Drive) vehicle, for which a possible distribution of the driving torque T_{shaft} [Nm], produced by the engine, and the brake torque T_{brake} [Nm], produced by the braking system, on the front and rear wheels is given by [5]:

$$T_F = 0.5T_{\text{shaft}} - 0.3T_{\text{brake}}, \tag{2a}$$
$$T_R = -0.2T_{\text{brake}}. \tag{2b}$$

The disturbance due to the rolling wheel resistance is given by $f_d = c_{\text{roll}}mg$, where c_{roll} is the rolling resistance coefficient and g [m/s^2] is the gravitational acceleration. Following [2, 6], the longitudinal forces acting on the front and rear tires are given by

$$f_F = \mu_F(\lambda_F)N_F, \qquad f_R = \mu_R(\lambda_R)N_R, \tag{3}$$

where $\mu_F(\lambda_F)$ and $\mu_R(\lambda_R)$ are the friction coefficients, while N_F and N_R are the normal loads on the front and rear wheels, respectively. Typically, $\mu_F(\lambda_F)$ and $\mu_R(\lambda_R)$ are nonlinear functions, depending on the slip ratios of the front and rear wheels λ_F and λ_R, respectively. Using the Bakker-Pacjeka model [1], we may assume that the friction coefficients depend on the slip ratios as follows

$$\mu_*(\lambda_*) = D_*\sin\Big(C_*\arctan(B_*\lambda_*)\Big), \quad * = F,R, \tag{4}$$

where B_*, C_*, and D_* are parameters fitting experimental data. For notational convenience, the argument in μ_F and μ_R will be dropped in the sequel. The normal loads N_F and N_R satisfy the following relations

$$N_F = mg\frac{l_R}{L} - \frac{h}{L}m\dot{v}, \quad N_R = mg\frac{l_F}{L} + \frac{h}{L}m\dot{v}, \quad N_F + N_R = mg, \tag{5}$$

with h [m] the vertical distance to the vehicle's center of mass, l_F [m] the distance from the front axle to the vehicle's center of mass, l_R [m] the distance from the rear axle to the vehicle's center of mass and L the distance from the front to the rear axle, given by $L = l_F + l_R$. As described in the next section, the vehicle has an intrinsic hybrid nature that leads to a hybrid model abstraction.

Hybrid Vehicle Model with Load Transfer

In this section, we use the formalism of hybrid systems [8] to model the longitudinal vehicle dynamics of a FWD vehicle, including the effect of longitudinal load transfer. We propose two different abstraction levels for the hybrid system modeling a FWD vehicle: the Vehicle-level Hybrid System (VHS) and the Wheel-level Hybrid System (WHS), as depicted in Figure 2. The difference between the two levels stems from the effects of the time delay between the driver's command (accelerate or brake) and the reactions of the wheels in the model description. For convenience of notation, in Figure 2 we denote with the superscript $\mathcal{V}$ the elements related to the VHS model abstraction and with superscript $\mathcal{W}$ the elements related to the WHS model abstraction. We will use the VHS model for designing the controller and the WHS for evaluating the efficiency of the designed hybrid controller. Both the abstraction levels are described using the following definitions of the wheels' and vehicle's operating conditions.

Definition 1: Wheel Modes. Given the wheels' slip ratios for a FWD vehicle [2]:

$$\lambda_F^d = \frac{r\omega_F^d - v^d}{r\omega_F^d} \quad \text{for} \quad v^d < r\omega_F^d, \tag{6a}$$
$$\lambda_R^d = 0 \quad \text{for} \quad v^d = r\omega_R^d, \tag{6b}$$
$$\lambda_F^b = \frac{r\omega_F^b - v^b}{v^b} \quad \text{for} \quad v^b > r\omega_F^b, \tag{6c}$$
$$\lambda_R^b = \frac{r\omega_R^b - v^b}{v^b} \quad \text{for} \quad v^b > r\omega_R^b, \tag{6d}$$

we say that the front (rear) wheel is in *wheel driving mode* if $\lambda_F^d \geq 0$ ($\lambda_R^d = 0$) and it is in *wheel braking mode* if $\lambda_F^b < 0$ ($\lambda_R^b < 0$), where the superscribed index d denotes the *driving mode* and the superscribed index b denotes the *braking mode* for the corresponding wheel.

Definition 2: Vehicle Modes. Given the total force acting between the vehicle's tires and the road as $f_{\text{tot}} = f_F + f_R - f_d$, we say that a vehicle is in *vehicle driving mode* if $f_{\text{tot}} \geq 0$ and in *vehicle braking mode* if $f_{\text{tot}} < 0$, where the forces (f_F^d, f_R^d) for the vehicle driving mode and (f_F^b, f_R^b) for the vehicle braking mode, given, respectively, by

$$f_F^d = \mu_F^d \Big(mg \frac{l_R}{L + h\mu_F^d} + \frac{h}{L + h\mu_F^d} f_d^d \Big), \tag{7a}$$

$$f_R^d = 0, \tag{7b}$$

$$f_F^b = \mu_F^b \Big(mg \frac{l_R - h\mu_R^b}{L + h(\mu_F^b - \mu_R^b)} + \frac{h}{L + h(\mu_F^b - \mu_R^b)} f_d^b \Big), \tag{7c}$$

$$f_R^b = \mu_R^b \Big(mg \frac{l_F + h\mu_F^b}{L + h(\mu_F^b - \mu_R^b)} - \frac{h}{L + h(\mu_F^b - \mu_R^b)} f_d^b \Big), \tag{7d}$$

where $f_d^d = f_d^b = f_d$ and

$$\mu_F^d = D_F \sin\Big(C_F \arctan(B_F \lambda_F^d) \Big), \quad \text{for} \quad 0 \leq \lambda_F^d \leq 1, \tag{8a}$$

$$\mu_R^d = 0, \quad \text{for} \quad \lambda_R^d = 0, \tag{8b}$$

$$\mu_F^b = D_F \sin\Big(C_F \arctan(B_F \lambda_F^b) \Big), \quad \text{for} \quad -1 \leq \lambda_F^b < 0, \tag{8c}$$

$$\mu_R^b = D_R \sin\Big(C_R \arctan(B_R \lambda_R^b) \Big), \quad \text{for} \quad -1 \leq \lambda_R^b < 0. \tag{8d}$$

Deriving and rearranging terms in (6) and using (1), and after denoting with $x = (v, \lambda_F, \lambda_R)^T$ the state of the vehicle in slip ratio variables, one obtains five dynamic systems, given by $\dot{x} = f_i^{\mathcal{W}}(x,u,d)$ ($i = 1,\ldots,5$)), which model the longitudinal vehicle behavior at the wheel level, as follows:

1. *Vehicle driving mode* ($f_{\text{tot}}^d \geq 0$) with wheels in *wheel driving/driving mode* ($\lambda_F^d \geq 0$ and $\lambda_R^d = 0$):

$$f_1^{\mathcal{W}}(x,u,d) = \begin{bmatrix} k_0\Big(f_F^d + f_R^d - f_d^d \Big) \\ -k_0\Big(\frac{f_F^d + f_R^d - f_d^d}{v^d} \Big)\gamma_F^d - k_1 \frac{f_F^d}{v^d}\eta_F^d + k_2 \frac{T_F^d}{v^d}\eta_F^d \end{bmatrix} \tag{9}$$

2. *Vehicle driving mode* ($f_{\text{tot}}^d \geq 0$) with wheels in *wheel driving/braking mode* ($\lambda_F^d \geq 0$ and $\lambda_R^b < 0$):

$$f_2^{\mathcal{W}}(x,u,d) = \begin{bmatrix} k_0\Big(f_F^d + f_R^b - f_d^d \Big) \\ -k_0\Big(\frac{f_F^d + f_R^d - f_d^d}{v^d} \Big)\gamma_F^d - k_1 \frac{f_F^d}{v^d}\eta_F^d + k_2 \frac{T_F^d}{v^d}\eta_F^d \\ -k_0\Big(\frac{f_F^b + f_R^b - f_d^b}{v^b} \Big)\gamma_R^b - k_3 \frac{f_R^b}{v^b} + k_4 \frac{T_R^b}{v^b} \end{bmatrix} \tag{10}$$

3. *Vehicle braking mode* ($f_{\text{tot}}^b < 0$) with wheels in *wheel driving/braking mode* ($\lambda_F^d \geq 0$ and $\lambda_R^b < 0$):

$$f_3^{\mathcal{W}}(x,u,d) = \begin{bmatrix} k_0\Big(f_F^d + f_R^b - f_d^b \Big) \\ -k_0\Big(\frac{f_F^d + f_R^d - f_d^d}{v^d} \Big)\gamma_F^d - k_1 \frac{f_F^d}{v^d}\eta_F^d + k_2 \frac{T_F^d}{v^d}\eta_F^d \\ -k_0\Big(\frac{f_F^b + f_R^b - f_d^b}{v^b} \Big)\gamma_R^b - k_3 \frac{f_R^b}{v^b} + k_4 \frac{T_R^b}{v^b} \end{bmatrix} \tag{11}$$

4. *Vehicle braking mode* ($f_{\text{tot}}^b < 0$) with wheels in *wheel braking/braking mode* ($\lambda_F^b < 0$ and $\lambda_R^b < 0$):

$$f_4^{\mathcal{W}}(x,u,d) = \begin{bmatrix} k_0\Big(f_F^b + f_R^b - f_d^b \Big) \\ -k_0\Big(\frac{f_F^b + f_R^b - f_d^b}{v^b} \Big)\gamma_F^b - k_1 \frac{f_F^b}{v^b} + k_2 \frac{T_F^b}{v^b} \\ -k_0\Big(\frac{f_F^b + f_R^b - f_d^b}{v^b} \Big)\gamma_R^b - k_3 \frac{f_R^b}{v^b} + k_4 \frac{T_R^b}{v^b} \end{bmatrix} \tag{12}$$

5. *Vehicle braking mode* ($f_{\text{tot}}^b < 0$) with wheels in *wheel braking/driving mode* ($\lambda_F^b < 0$ and $\lambda_R^d = 0$):

$$f_5^{\mathcal{W}}(x,u,d) = \begin{bmatrix} k_0\Big(f_F^b + f_R^d - f_d^b \Big) \\ -k_0\Big(\frac{f_F^b + f_R^b - f_d^b}{v^b} \Big)\gamma_F^b - k_1 \frac{f_F^b}{v^b} + k_2 \frac{T_F^b}{v^b} \end{bmatrix} \tag{13}$$

where $k_0 = 1/m$, $k_1 = r^2/I_F$, $k_2 = r/I_F$, $k_3 = r^2/I_R$, $k_4 = r/I_R$ and $\eta_F^d = (1 - \lambda_F^d)^2$, $\gamma_F^d = (1 - \lambda_F^d)$, $\gamma_F^b = (1 + \lambda_F^b)$, and $\gamma_R^b = (1 + \lambda_R^b)$.

At this level, we assumed that both engine and brake torques do not have an immediate effect on the wheels, but there is a time delay between the driver's command (accelerating or braking) and the effective reactions on the wheels. Using the notation described in [8], each of these five models corresponds to a discrete state $q^{\mathcal{W}} \in Q^{\mathcal{W}} = \{q_1^{\mathcal{W}}, q_2^{\mathcal{W}}, q_3^{\mathcal{W}}, q_4^{\mathcal{W}}, q_5^{\mathcal{W}}\}$ of a finite state automaton as depicted at the bottom in Figure 2: two for the vehicle driving mode ($q_1^{\mathcal{W}}$ and $q_2^{\mathcal{W}}$) referring to a total friction force being nonnegative, and three for the vehicle braking mode ($q_3^{\mathcal{W}}$ and $q_4^{\mathcal{W}}$ and $q_5^{\mathcal{W}}$), where the total friction force is negative. The state $q_1^{\mathcal{W}}$ corresponds to (front and rear) wheels with friction slip ratios nonnegative, and $q_4^{\mathcal{W}}$ corresponds to (front and rear)

wheels with friction slip ratios negative. The rest of the states ($q_2^{\mathcal{W}}$, $q_3^{\mathcal{W}}$, $q_5^{\mathcal{W}}$) describes mixed operating conditions, in which front and rear wheels have slip ratios with different signs. The transitions among these five models are regulated by the guard conditions $G_{12}^{\mathcal{W}}$, $G_{23}^{\mathcal{W}}$, $G_{34}^{\mathcal{W}}$, $G_{45}^{\mathcal{W}}$, $G_{51}^{\mathcal{W}}$, which are forced when the invariant conditions are violated. After a transition, the state x can be reset through the reset functions ($R_{12}^{\mathcal{W}}$, $R_{23}^{\mathcal{W}}$, $R_{34}^{\mathcal{W}}$ and $R_{45}^{\mathcal{W}}$, $R_{51}^{\mathcal{W}}$) described in Figure 2.

At the VHS level, we assume that the time delay between the driver's command to accelerate (brake) and the reactions of

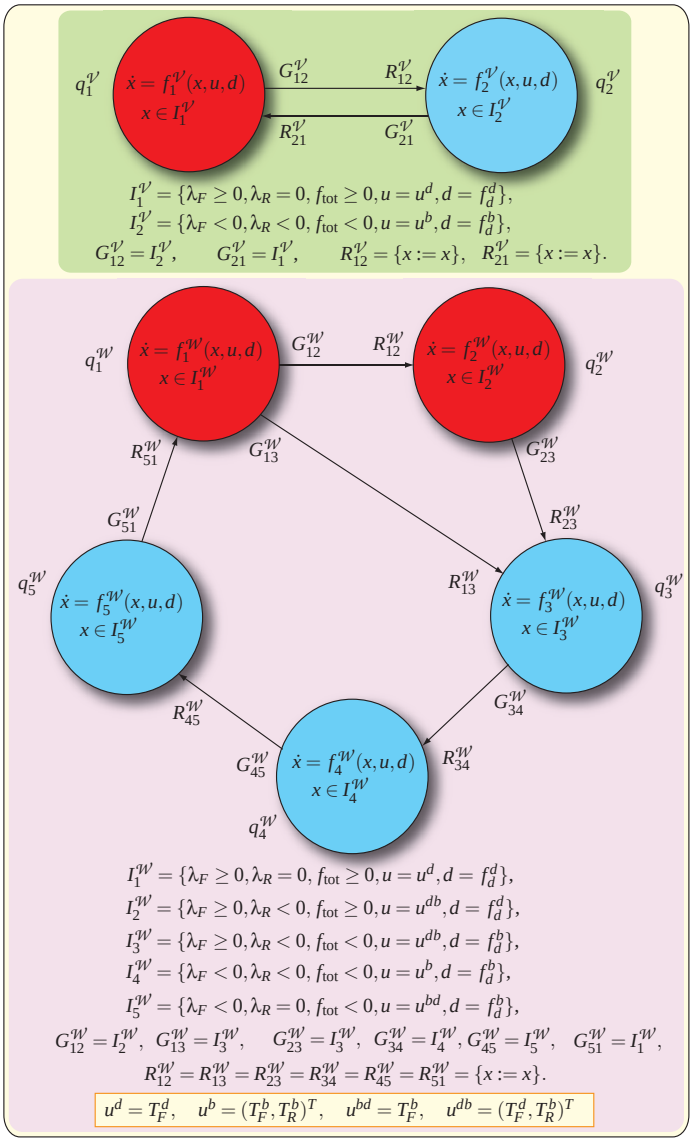

Figure 2. GRAPHICAL REPRESENTATION OF THE HYBRID SYSTEM MODELING THE LONGITUDINAL VEHICLE DYNAMICS AT VEHICLE ($\mathcal{V}$) AND WHEEL ($\mathcal{W}$) LEVEL.

the wheels (front and rear) is zero. This allows a description at a higher level of abstraction of the vehicle through two models, each corresponding to a state $q^{\mathcal{V}} \in Q^{\mathcal{V}} = \{q_1^{\mathcal{V}}, q_2^{\mathcal{V}}\}$ of a finite state automaton as depicted at the top of Figure 2: one for the vehicle driving mode ($q_1^{\mathcal{V}}$) and one for the vehicle braking mode ($q_2^{\mathcal{V}}$). The transitions among these models, depending on the value of the system state described by (9) and (12), are regulated by the guard conditions ($G_{12}^{\mathcal{V}}$, $G_{21}^{\mathcal{V}}$), stating when a transition can take place. They are forced when the invariant conditions ($x \in I_1^{\mathcal{V}}$, $x \in I_2^{\mathcal{V}}$) are violated. The reset functions are $R_{12}^{\mathcal{V}}$, $R_{21}^{\mathcal{V}}$. The VHS and the WHS models are connected through the following relations $q_1^{\mathcal{V}} \equiv q_1^{\mathcal{W}}$ and $q_2^{\mathcal{V}} \equiv q_4^{\mathcal{W}}$ and consequently $f_1^{\mathcal{V}}(x,u,d) = f_1^{\mathcal{W}}(x,u,d)$ and $f_2^{\mathcal{V}}(x,u,d) = f_4^{\mathcal{W}}(x,u,d)$.

Control Problem Formulation

In this section we formulate the control problem for the vehicle-level hybrid system ((9), (12)) to determine a hybrid controller such that the vehicle accelerates or brakes following a prescribed reference friction force $f_{\text{tot}}^{\text{ref}}(t)$, while the (known) disturbances are rejected. This problem can be solved using the nonlinear output regulation theory [4], where the reference and the disturbance are produced by an autonomous dynamic system, called the "exosystem," given by

$$\begin{pmatrix} \dot{w}_1 \\ \dot{w}_2 \\ \dot{w}_3 \\ \dot{w}_4 \end{pmatrix} = \begin{pmatrix} 0 & -\omega_e & 0 & 0 \\ \omega_e & 0 & 0 & 0 \\ 0 & 0 & 0 & 0 \\ 0 & 0 & 0 & 0 \end{pmatrix} \begin{pmatrix} w_1 \\ w_2 \\ w_3 \\ w_4 \end{pmatrix}, \tag{14}$$

with initial conditions $w(0) = (w_1(0), w_2(0), w_3(0), w_4(0))^{\mathrm{T}} = (1, 0, v_0, \mathrm{mg})^{\mathrm{T}}$, where ω_e [rad/s] is the known frequency of the reference signal and v_0 [m/s] is the initial vehicle velocity. We consider a reference trajectory such that the total traction friction force is nonnegative for vehicle driving mode and strictly negative for vehicle braking mode. Denoting with $f_F^{d,\text{ref}}(w)$ the reference friction force of the front wheel for driving, and with $f_F^{b,\text{ref}}(w)$ and $f_R^{b,\text{ref}}(w)$ the reference friction force of the front and rear wheel for braking, respectively, we define the reference trajectories as a combination of sinusoidal signals:

$$f_F^{d,\text{ref}}(w) = \sum_{i=1}^{4} a_i w_i, \; f_F^{b,\text{ref}}(w) = \sum_{i=1}^{4} b_i w_i, \; f_R^{b,\text{ref}}(w) = \sum_{i=1}^{4} c_i w_i, \tag{15}$$

where the coefficients a_i, b_i, c_i, $i = 1, \cdots, 4$ are determined such that the physical constraints of friction forces are satisfied. Here, we have $a_1 \leq f_F^{d,\max} - c_{\text{roll}} mg$, $b_1 \leq f_F^{b,\max} - (c_{\text{roll}}/2) mg$, $c_1 \leq f_R^{b,\max} - (c_{\text{roll}}/2) mg$, where $f_F^{d,\max}$, $f_F^{b,\max}$, and $f_R^{b,\max}$ are derived from (7) and $a_2 = a_3 = b_2 = b_3 = c_2 = c_3 = 0$, $a_4 = c_{\text{roll}}$, $b_4 =$

$c_4 = c_{\text{roll}}/2$. The disturbance $f_d(w)$ acting on the system is

$$f_d(w) = a_4 w_4. \tag{16}$$

After setting $e^d = e^d_F$ and $e^b = (e^b_F, e^b_R)^T$, the output error equations for the vehicle driving mode and the vehicle braking mode are:

$$\begin{aligned} e^d &= \left(f^d_F - f^{d,\text{ref}}_F(w) \right) = h^{\mathcal{V}}_1(x,w), \\ e^b &= \begin{pmatrix} f^b_F - f^{b,\text{ref}}_F(w) \\ f^b_R - f^{b,\text{ref}}_R(w) \end{pmatrix} = h^{\mathcal{V}}_2(x,w). \end{aligned} \tag{17}$$

The control problem is then formulated as follows. Given the high-level hybrid system model of the longitudinal vehicle dynamics (top of Figure 2) of the form

$$\begin{aligned} \dot{x} &= f^{\mathcal{V}}_1(x,u,w), \qquad \dot{x} = f^{\mathcal{V}}_2(x,u,w), \\ e^d &= h^{\mathcal{V}}_1(x,w), \qquad e^b = h^{\mathcal{V}}_2(x,w), \end{aligned} \tag{18}$$

with its invariants $I^{\mathcal{V}}_1$ and $I^{\mathcal{V}}_2$, respectively, as reported in Figure 2, and with nominal values of their linear parts around the equilibrium point $(x_0, 0, 0)$

$$\begin{aligned} A^d_0 &= \left.\frac{\partial f^{\mathcal{V}}_1}{\partial x}\right|_{(x_0,0,0)}, \quad B^d_0 = \left.\frac{\partial f^{\mathcal{V}}_1}{\partial u}\right|_{(x_0,0,0)}, \quad C^d_0 = \left.\frac{\partial h^{\mathcal{V}}_1}{\partial x}\right|_{(0,0)}, \\ A^b_0 &= \left.\frac{\partial f^{\mathcal{V}}_2}{\partial x}\right|_{(x_0,0,0)}, \quad B^b_0 = \left.\frac{\partial f^{\mathcal{V}}_2}{\partial u}\right|_{(x_0,0,0)}, \quad C^b_0 = \left.\frac{\partial h^{\mathcal{V}}_2}{\partial x}\right|_{(0,0)}, \end{aligned} \tag{19}$$

where the initial state x_0 is given by $x_0 = (v_0, 0, 0)^T$ and the pairs (A^d_0, B^d_0), (A^b_0, B^b_0) are stabilizable, and given an autonomous linear system, Poisson stable, $\dot{w} = Sw$ with $w(0) \in W^o \subset \mathbb{R}^4$ (with W^o neighborhood of the equilibrium point), generating (17), design controllers of the form

$$\alpha^d(x,w) = c^d(w) + K^d(x - \pi^d(w)), \tag{20a}$$
$$\alpha^b(x,w) = c^b(w) + K^b(x - \pi^b(w)), \tag{20b}$$

where $x = \pi^d(w) \in I^{\mathcal{V}}_1 \subset \mathbb{R}^2$ and $x = \pi^b(w) \in I^{\mathcal{V}}_2 \subset \mathbb{R}^3$ with $\pi^d(0) = \pi^b(0) = 0$ are the steady-state zero output manifolds, and where $u = c^d(w) \in I^{\mathcal{V}}_1 \subset \mathbb{R}$ and $u = c^b(w) \in I^{\mathcal{V}}_2 \subset \mathbb{R}^2$ with $c^d(0) = c^b(0) = 0$ are the steady-state control inputs, for driving and braking dynamics, respectively, with K^d and K^b matrices such that the eigenvalues of $(A^d_0 + B^d_0 K^d)$ and $(A^b_0 + B^b_0 K^b)$ are in the open left-half complex plane and such that the *regulator equations*:

$$\begin{aligned} \frac{\partial \pi^d}{\partial w} Sw &= f^{\mathcal{V}}_1(\pi^d(w), c^d(w), w), \qquad \frac{\partial \pi^b}{\partial w} Sw = f^{\mathcal{V}}_2(\pi^b(w), c^b(w), w), \\ 0 &= h^{\mathcal{V}}_1(\pi^d(w), w), \qquad 0 = h^{\mathcal{V}}_2(\pi^b(w), w), \end{aligned} \tag{21}$$

are satisfied for all $w \in W^o$ and for all admissible values of the parameters of the plant and the exosystem.

CONTROL LAW DESIGN

We design the hybrid regulator for the tracking of the traction friction forces of a longitudinal vehicle model in its hybrid formulation (Figure 2) using the nonlinear output regulation [4].

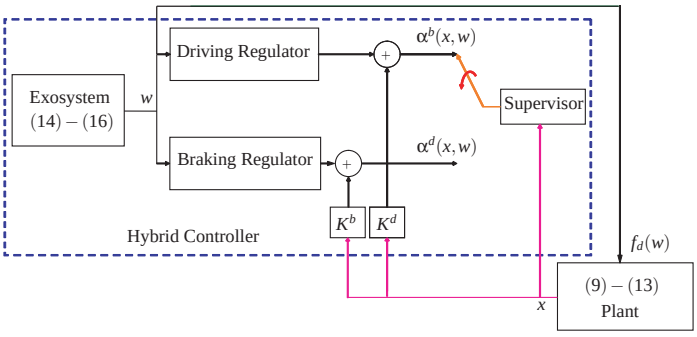

Figure 3. HYBRID REGULATOR SCHEME OF LONGITUDINAL VEHICLE DYNAMICS WITH LOAD TRANSFER EFFECTS.

Vehicle Driving Regulator

We solve the regulator equation (22) for the vehicle driving mode.

$$\begin{aligned} \frac{\partial \pi_{v^d}}{\partial w} S &= k_0(\pi_{f^d_F} + \pi_{f^d_R} - \pi_{f^d_d}) \\ \frac{\partial \pi_{\lambda^d_F}}{\partial w} S &= -k_0 \left(\frac{\pi_{f^d_F} + \pi_{f^d_R} - \pi_{f^d_d}}{\pi_{v^d}} \right) \pi_{\lambda^d_F} - k_1 \left(\frac{\pi_{f^d_F}}{\pi_{v^d}} \right) \eta^d_F + k_2 \left(\frac{c_{u^d_F}}{\pi_{v^d}} \right) \eta^d_F \\ 0 &= \pi_{f^d_F} - f^{d,ref}_F. \end{aligned} \tag{22}$$

Given (23), we compute the steady-state zero output manifold $\pi^d(w) = (\pi_{v^d}, \pi_{\lambda^d_F})^T$ and the steady-state input $c^d(w) = c_{u^d_F}$, as follows

$$\pi_{v^d} = v^d|_{x=\pi^d(w)}, \tag{23a}$$
$$\pi_{f^d_d} = f^d_d|_{x=\pi^d(w)} = a_4 w_4, \tag{23b}$$
$$c_{u^d_F} = u^d_F|_{u=c^d(w)}, \tag{23c}$$
$$\pi_{\mu^d_F} = D_F \sin(C_F \arctan(B_F \pi_{\lambda^d_F})), \tag{23d}$$

and

$$\pi_{N_F^d} = N_F^d|_{x=\pi^d(w)} = mg\frac{l_R}{L} - \frac{h}{L}m\dot{\pi}_{v^d}, \tag{24a}$$

$$\pi_{f_F^d} = f_F^d|_{x=\pi^d(w)} = \pi_{\mu_F^d}\pi_{N_F^d}, \tag{24b}$$

$$\pi_{\gamma_F^d} = \gamma_F^d|_{x=\pi^d(w)} = (1-\pi_{\lambda_F^d}), \tag{24c}$$

$$\pi_{\eta_F^d} = \eta_F^d|_{x=\pi^d(w)} = (1-\pi_{\lambda_F^d})^2 \tag{24d}$$

From the last equation of (22), one obtains $\pi_{f_F^d} = f_F^{d,\text{ref}}$, and after substituting this together with (15), (16), (23b), (24b) in the first equation of (22), one obtains $\frac{\partial \pi_{v^d}}{\partial w}S = \frac{a_1 w_1}{m}$, whose solution is $\pi_v^d = \alpha w_2 + w_3$ with $\alpha = a_1/m\omega_e$. By inversion of (23d), one obtains

$$\pi_{\lambda_F^d} = p_0 \tan(p_1 \arcsin(p_3(\pi_{\mu_F^d}))), \tag{25}$$

after combining (24a) and (24b). Given the previous expressions of $\pi_{f_F^d}$ and $\dot{\pi}_{v^d}$, one gets $\pi_{\mu_F^d}$ of the form

$$\pi_{\mu_F^d} = L\frac{a_1 w_1 + a_4 w_4}{mgl_R - ha_1 w_1}. \tag{26}$$

From the second equation of (22), one gets the steady-state control input $c_{u_F^d}$ (control input of front wheel):

$$c_{u_F^d} = \frac{I_F}{r}\frac{\pi_{v^d}}{(1-\pi_{\lambda_F^d})^2}L_s\pi_{\lambda_F^d} + \frac{I_F}{r}\frac{1}{m}\left(\frac{\pi_{f_F^d} - \pi_{f_d^d}}{1-\pi_{\lambda_F^d}}\right) + r\pi_{f_{F^d}} \tag{27}$$

with $L_s\pi_{\lambda_F^d} = \frac{\partial \pi_{\lambda_F^d}}{\partial w}S = Lp_0p_1p_2\sigma_F^d\rho_F^d$, where

$$\sigma_F^d = \frac{1}{\cos^2(p_1\arcsin(p_2\pi_{\mu_F^d}))}\frac{1}{(1-(p_2\pi_{\mu_F^d})^2)^{1/2}}\frac{1}{(mgl_R - ha_1w_1)^2}, \tag{28}$$

and $\rho_F^d = -\omega_e a_1(mgl_R + ha_4w_4)w_2$. Finally, the steady-state solution and the feedback control law for the vehicle driving mode are

$$\pi^d(w) = \begin{pmatrix} \alpha w_2 + w_3 \\ p_0\tan(p_1\arcsin(p_2\pi_{\mu_F^d})) \end{pmatrix}, \tag{29a}$$

$$c^d(w) = \frac{I_F}{r}\frac{\pi_{v^d}}{(1-\pi_{\lambda_F^d})^2}L_s\pi_{\lambda_F^d} + \frac{I_F}{r}\frac{1}{m}\left(\frac{\pi_{f_F^d} - \pi_{f_d^d}}{1-\pi_{\lambda_F^d}}\right) + r\pi_{f_{F^d}}, \tag{29b}$$

along with (20a), where K^d is designed based on the linearized vehicle driving mode around the equilibrium point $(x_0, 0, 0)$ with $x_0 = (v_0, 0, 0)^T$ and described by the matrices A_0^d, B_0^d, C_0^d in the Appendix.

Vehicle Braking Regulator

We compute the steady-state zero output manifold $\pi^b(w) = (\pi_{v^b}, \pi_{\lambda_F^b}, \pi_{\lambda_R^b})^T$ and the steady-state input $c^b(w) = (c_{u_F^b}, c_{u_R^b})^T$ for the vehicle braking mode, solving the regulator equation (30)

$$\begin{aligned}
&\frac{\partial \pi_{v^b}}{\partial w}S = k_0(\pi_{f_F^b} + \pi_{f_R^b} - \pi_{f_d^b}) \\
&\frac{\partial \pi_{\lambda_F^b}}{\partial w}S = -k_0(1+\pi_{\lambda_F^b})\left(\frac{\pi_{f_F^b} + \pi_{f_R^b} - \pi_{f_d^b}}{\pi_{v^b}}\right) - k_1\left(\frac{\pi_{f_F^b}}{\pi_{v^b}}\right) + k_2\left(\frac{c_{u_F^b}}{\pi_{v^b}}\right) \\
&\frac{\partial \pi_{\lambda_R^b}}{\partial w}S = -k_0(1+\pi_{\lambda_R^b})(\frac{\pi_{f_F^b} + \pi_{f_R^b} - \pi_{f_d^b}}{\pi_{v^b}}) - k_3\left(\frac{\pi_{f_R^b}}{\pi_{v^b}}\right) + k_4\left(\frac{c_{u_R^b}}{\pi_{v^b}}\right) \\
&\begin{pmatrix} 0 \\ 0 \end{pmatrix} = \begin{pmatrix} \pi_{f_F^b} - f_F^{b,ref} \\ \pi_{f_R^b} - f_R^{b,ref} \end{pmatrix}.
\end{aligned} \tag{30}$$

The terms of (30) are defined as

$$\pi_{v^b} = v^b|_{x=\pi^b(w)}, \quad \pi_{f_d^b} = f_d^b|_{x=\pi^b(w)} = a_4w_4, \tag{31a}$$

$$c_{u_F^b} = u_F^b|_{u=c^b(w)}, \quad c_{u_R^b} = u_R^b|_{u=c^b(w)}, \tag{31b}$$

$$\pi_{\mu_F^b} = D_F\sin(C_F\arctan(B_F\pi_{\lambda_F^b}), \tag{31c}$$

$$\pi_{\mu_R^b} = D_R\sin(C_R\arctan(B_R\pi_{\lambda_R^b}), \tag{31d}$$

$$\pi_{N_F^b} = N_F^b|_{x=\pi^b(w)} = mg\frac{l_R}{L} - \frac{h}{L}m\dot{\pi}_{v^b}, \tag{31e}$$

$$\pi_{N_R^b} = N_R^b|_{x=\pi^b(w)} = mg\frac{l_F}{L} + \frac{h}{L}m\dot{\pi}_{v^b}, \tag{31f}$$

$$\pi_{f_F^b} = f_F^b|_{x=\pi^b(w)} = (\pi_{\mu_F^b})(\pi_{N_F^b}), \tag{31g}$$

$$\pi_{f_R^b} = f_R^b|_{x=\pi^b(w)} = (\pi_{\mu_F^b})(\pi_{N_F^b}). \tag{31h}$$

Analogously to the vehicle driving mode, we find the solution of (30), given by

$$\pi_{v^b} = \beta w_2 + w_3, \quad \pi_{\lambda_F^b} = q_0\tan(\vartheta_1), \quad \pi_{\lambda_R^b} = z_0\tan(\vartheta_2), \tag{32}$$

where $\vartheta_1 = q_1\arcsin(q_2\pi_{\mu_F^b})$, $\vartheta_2 = z_1\arcsin(p_2\pi_{\mu_R^b})$, and

$$\begin{aligned}
c_{u_F^b} &= \frac{I_F}{r}\pi_{v^b}L_s\pi_{\lambda_{Fb}} + \frac{I_F}{r}\frac{1}{m}(1+\pi_{\lambda_{Fb}})(\pi_{f_F^b} + \pi_{f_R^b} - \pi_{f_d^b}) + r\pi_{f_{Fb}}, \\
c_{u_R^b} &= \frac{I_R}{r}\pi_{v^b}L_s\pi_{\lambda_{Rb}} + \frac{I_R}{r}\frac{1}{m}(1+\pi_{\lambda_{Rb}})\left(\pi_{f_F^b} + \pi_{f_R^b} - \pi_{f_d^b}\right) + r\pi_{f_{Rb}},
\end{aligned} \tag{33}$$

where

$$\pi_{\mu_F^b} = L\frac{b_1 w_1 + b_4 w_4}{mgl_R - h(b_1+c_1)w_1}, \quad L_s\pi_{\lambda_F^b} = \frac{\partial \pi_{\lambda_F^b}}{\partial w} S = Lq_0 q_1 q_2 \sigma_F^b \rho_F^b,$$

$$\pi_{\mu_R^b} = L\frac{c_1 w_1 + c_4 w_4}{mgl_F + h(c_1+b_1)w_1}, \quad L_s\pi_{\lambda_R^b} = \frac{\partial \pi_{\lambda_R^b}}{\partial w} S = Lz_0 z_1 z_2 \sigma_R^b \rho_R^b,$$

with

$$\begin{aligned}
\rho_F^b &= -\omega_e(mgl_R b_1 - hb_4(b_1+c_1)w_4)w_2, \\
\rho_R^b &= \omega_e(mgl_F c_1 + hc_4(b_1+c_1)w_4)w_1, \\
\sigma_F^b &= \frac{1}{\cos^2(\vartheta_1)} \frac{1}{(1-(p_2\pi_{\mu_F^b})^2)^{1/2}} \frac{1}{(mgl_R - h(b_1+c_1)w_1)^2}, \\
\sigma_R^b &= \frac{1}{\cos^2(\vartheta_2)} \frac{1}{(1-(z_2\pi_{\mu_R^b})^2)^{1/2}} \frac{1}{(mgl_F + h(b_1+c_1)w_1)^2},
\end{aligned} \tag{34}$$

with $\beta = (b_1+c_1)/m\omega_e$, $q_0 = 1/B_F$, $q_1 = 1/C_F$, $q_2 = 1/D_F$, $z_0 = 1/B_R$, $z_1 = 1/C_R$, $z_2 = 1/D_R$. The feedback control law for the *vehicle braking mode* is given by (20(b)) where K^b is designed based on the linearized vehicle braking dynamics around the equilibrium point $(x_0, 0, 0)$ with $x_0 = (v_0, 0, 0)^T$ and described by the matrices A_0^b, B_0^b, C_0^b in the Appendix.

NUMERICAL RESULTS

In this section, we present simulation results, given in MATLAB, concerning a specific model of a vehicle, with the following nominal parameters (extracted from the "Big Sedan" vehicle in CarSim): $m = 853.5$ kg, $I_F = I_R = 0.9$ kgm^2, $h = 0.515$ m, $l_F = 1.033$ m, $l_R = 1.657$ m, $r = 0.278$ m, $c_{\text{roll}} = 0.01$, $B = 7$, $C = 1.6$, $D = 0.8$. The reference friction forces on the front and rear wheel $f_F^{\text{ref}}(t)$ and $f_R^{\text{ref}}(t)$ and the disturbance $f_d(t)$ are assumed to be generated by a four-dimensional neutrally stable exosystem, with parameters $\omega_e = 1$ [rad/s] and initial conditions $w(0) = (w_1(0), w_2(0), w_3(0), w_4(0))^T = (1, 0, 15\,[\text{m/s}], 8373\,[\text{N}])^{\text{T}}$. Furthermore, the coefficients of the reference friction forces have been set to $a_1 = 0.65 f_F^{d,\max} = 2333$ [N], $b_1 = 0.30 f_F^{b,\max} = 934$ [N], $c_1 = 0.50 f_R^{b,\max} = 1793$ [N]. Following Section IV, the controller is designed, for each operating condition, on the basis of the vehicle model described by the VHS ((9), (12)), and the simulations are performed on the full nonlinear vehicle model described by the WHS ((9)-(13)). In this way, we obtain the regulation for the regulation error $e(t)$, by the following suitable choice of the control parameters:

$$K^d = \begin{pmatrix} k_1^d & k_2^d \end{pmatrix} = -\begin{pmatrix} 7587 & 11983 \end{pmatrix} \tag{35a}$$

$$K^b = \begin{pmatrix} k_1^b & k_2^b & k_3^b \\ k_4^b & k_5^b & k_6^b \end{pmatrix} = -\begin{pmatrix} 953 & 12683 & 1109 \\ 594 & 1175 & 6800 \end{pmatrix}. \tag{35b}$$

Figure 4 presents simulation results for initial conditions $(v(0), \omega_F(0), \omega_R(0)) = (15.25\,[\text{m/s}], 70\,[\text{rad/s}], 54.85\,[\text{rad/s}])$. The figure shows the tracking of reference friction forces $f_F^{ref}(t)$ and $f_R^{\text{ref}}(t)$ (first row of figure) and the related tracking errors (second row of figure). Starting from an initial mismatch of the current friction force with the desired friction force of the front wheel, the friction force tracking error of the front wheel reaches zero around $t = 0.5$ s. In the third row of Figure 4 the two control variables T_{shaft} and T_{brake}, with the related switching variables λ_F and λ_R, are reported. It is clear that the controller allows

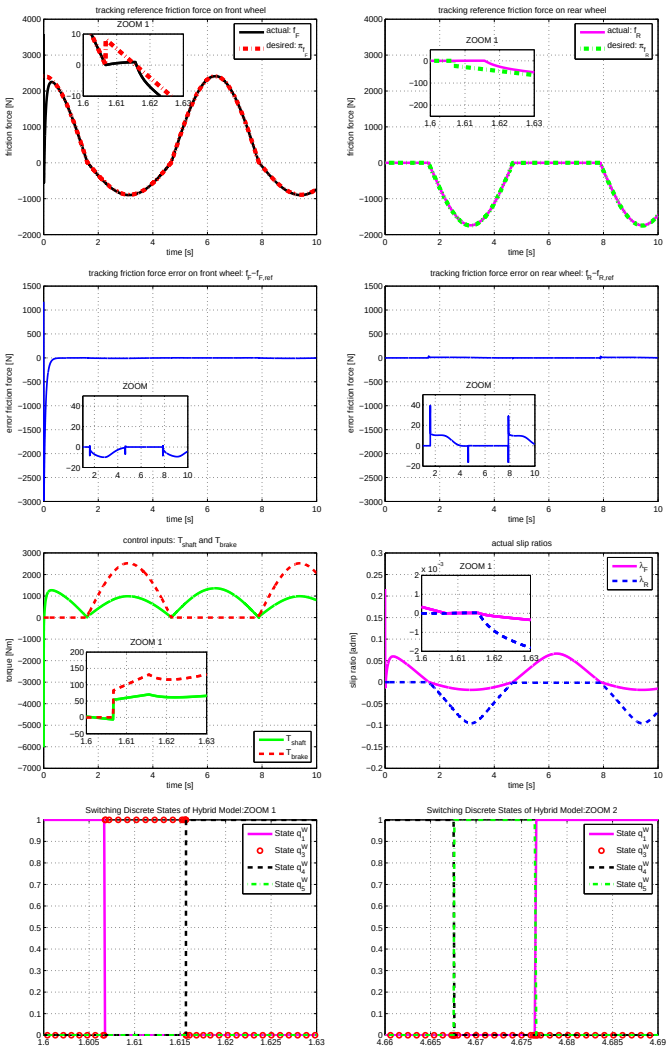

Figure 4. REGULATION OF FRICTION FORCES FOR A VEHICLE MODEL: tracking friction forces on front $f_F^{\text{ref}}(t)$ and rear $f_R^{\text{ref}}(t)$ wheels (first row), tracking errors $f_F(t) - f_F^{\text{ref}}(t)$, $f_R(t) - f_R^{\text{ref}}(t)$ (second row), control inputs T_{shaft}, T_{brake} and slip ratios $\lambda_F(t)$, $\lambda_R(t)$ (third row) and, switching from $q_1^{\mathcal{W}}$ to $q_4^{\mathcal{W}}$ via $q_3^{\mathcal{W}}$ (left, fourth row) and switching from $q_4^{\mathcal{W}}$ to $q_1^{\mathcal{W}}$ via $q_5^{\mathcal{W}}$ (right, fourth row) .

the tracking of reference friction forces and the stabilization of the vehicle despite known disturbances acting on model and unknown model uncertainties. Finally, in the last row of Fig. 4 the switching signals between $q_1^{\mathcal{W}}$ and $q_4^{\mathcal{W}}$ of the automaton of Fig. 2 are shown. As can be easily verified, the intermediate states $q_3^{\mathcal{W}}$ and $q_5^{\mathcal{W}}$ are indeed transient, having a very short duration.

CONCLUSIONS AND FUTURE WORK

We have applied the nonlinear output regulation theory to the design of a state-feedback vehicle control system, incorporating expert driving skills (ie, left foot braking) to adjust traction friction forces. Specifically, we considered the left-foot braking, where the load transfer effect plays a strategic role for accident avoidance in hazard scenarios. A longitudinal FWD vehicle model with load transfer dynamics has been derived and its formulation using hybrid models has been proposed. The designed hybrid controller, described in Figure 3, is given by a vehicle driving regulator $\alpha^d(x,w)$, which computes, through (29), the control input torque for the front wheel during the *vehicle driving mode* and, a vehicle braking regulator $\alpha^b(x,w)$, which computes, through (32), the control input torques for the front and rear wheels during the *vehicle braking mode*. The hybrid controller depends on eight design parameters (k_i^d with $i=1,2$ and k_j^b with $j=1,\cdots,6$.) We verified, via numerical simulations that, given a large compact set of initial conditions, it is possible to tune the design parameters in to achieve the desired control objective despite known disturbances and unknown model uncertainties. High-fidelity numerical simulations (using CarSim) of the presented algorithm are under investigation.

ACKNOWLEDGMENT

The authors gratefully acknowledge Ford Motor Company for their technical and financial support under the URP program. In addition, the first two authors would like to acknowledge the financial support from the US DoD SAVE program (contract no. 0603734A) and the NSF GOALI program (CMMI 0727768).

REFERENCES

[1] E. Bakker, L. Nyborg and H. B. Pacejka, "Tyre modelling for use in vehicle dynamics studies," *Proceedings of Society of Automotive Engineers international congress and exposition*, (Deatroit, Michigan), February 23, 1987.

[2] C. Canudas de Wit, P. Tsiotras, E. Velenis, M. Basset, and G. Gissinger, "Dynamic friction models for road-tire longitudinal interaction," *Vehicle System Dynamics*, vol. 39, no. 3, pp. 189-226, 2003.

[3] T. D. Gillespie, *Fundamentals of Vehicle Dynamics*. International Society of Automotive Engineers, Warrendale, PA, USA, 1992.

[4] A. Isidori, *Nonlinear Control Systems*. Springer-Verlag, London, UK, 1995.

[5] H. Lee and M. Tomizuka, "Adaptive vehicle traction force control for intelligent vehicle highway systems (IVHSs)," *IEEE Transactions on Industrial Electronics*, vol. 50, no. 1, pp. 37-47, February 2003.

[6] R. N. Jazar, *Vehicle Dynamics: Theory and Application*. Springer, 2008.

[7] A. Scacchioli, *Hybrid Regulation of Electromagnetic Valves in Automotive Systems*. EECS PhD thesis, University of L'Aquila, Italy, May 2005.

[8] C. J. Tomlin, J. Lygeros and S. S. Sastry, "A game theoretic approach to controller design for hybrid systems," in *Proceedings of the IEEE*, vol. 88, no. 7, pp. 949-970, July 2000.

[9] E. Velenis and P. Tsiotras, "Minimum time travel for a vehicle with acceleration limits: theoretical analysis and receding horizon implementation," in *Journal of Optimization Theory and Applications*, vol. 138, no. 2, pp. 275-296, August 2008.

[10] E. Velenis. P. Tsiotras and J. Lu, "Optimality Properties and Driver Input Parameterization for Trail-Braking Cornering," *European Journal of Control*, vol. 14, no. 4, pp. 308–320, 2008.

Appendix

$$A_0^d = \begin{pmatrix} a_{11}^d & a_{12}^d \\ a_{21}^d & a_{22}^d \end{pmatrix}, \quad B_0^d = \begin{pmatrix} b_{11}^d \\ b_{21}^d \end{pmatrix}, \quad C_0^d = \begin{pmatrix} c_{11}^d & c_{12}^d \end{pmatrix},$$

$$A_0^b = \begin{pmatrix} a_{11}^b & a_{12}^b & a_{13}^b \\ a_{21}^b & a_{22}^b & a_{23}^b \\ a_{31}^b & a_{32}^b & a_{33}^b \end{pmatrix}, \; B_0^b = \begin{pmatrix} b_{11}^b & b_{12}^b \\ b_{21}^b & b_{22}^b \\ b_{31}^b & b_{32}^b \end{pmatrix}, \; C_0^b = \begin{pmatrix} c_{11}^b & c_{12}^b & c_{13}^b \end{pmatrix}$$

with $a_{11}^d = -\frac{g}{v_0}\frac{l_R}{L}C_{fa,F}$, $a_{12}^d = g\frac{l_R}{L}C_{fa,F}$, $a_{21}^d = \frac{g}{v_0^2}\frac{l_R}{L}\Big(1 + r^2\frac{m}{I_F}\Big)C_{fa,F}$, $a_{22}^d = -\frac{g}{v_0}\frac{l_R}{L}\Big(1 + r^2\frac{m}{I_F}\Big)C_{fa,F}$, $b_{11}^d = c_{12}^d = 0$, $b_{21}^d = \frac{1}{v_0}\frac{r}{I_F}$, $c_{11}^d = 1$, $a_{11}^b = -\frac{1}{v_0^2}\frac{g}{L}\Big(C_{fa,F}l_R + C_{fa,R}l_F\Big)$, $a_{12}^b = \frac{g}{L}C_{fa,F}l_R$, $a_{13}^b = \frac{g}{L}C_{fa,R}l_F$, $a_{21}^b = \frac{1}{v_0^3}\frac{g}{L}\Big(C_{fa,F}l_R\Big(1 + r^2\frac{m}{I_F}\Big) + C_{fa,R}l_F\Big)$, $a_{22}^b = -\frac{g}{v_0}\frac{l_R}{L}C_{fa,F}\Big(1 + r^2\frac{m}{I_F}\Big)$, $a_{23}^b = -\frac{g}{v_0}\frac{l_F}{L}C_{fa,R}$, $a_{31}^b = \frac{1}{v_0^3}\frac{g}{L}\Big(C_{fa,F}l_R + C_{fa,R}l_F\Big(1 + r^2\frac{m}{I_R}\Big)\Big)$, $a_{32}^b = -\frac{g}{v_0}\frac{l_R}{L}C_{fa,F}$, $a_{33}^b = -\frac{g}{v_0}\frac{l_F}{L}C_{fa,R}\Big(1 + r^2\frac{m}{I_R}\Big)$, $b_{11}^b = b_{31}^b = b_{12}^b = b_{22}^b = c_{12}^b = c_{13}^b = 0$, $b_{21}^b = \frac{1}{v_0}\frac{r}{I_F}$, $b_{32}^b = \frac{1}{v_0}\frac{r}{I_R}$, $c_{11}^b = 1$, where $C_{fa,F} = B_F C_F D_F$, $C_{fa,R} = B_R C_R D_R$ and $v_0 = v(0)$.